

## Fuel cell drive system with hydrogen generation in test

B. Emonts<sup>a,\*</sup>, J. Bøgild Hansen<sup>b</sup>, H. Schmidt<sup>c</sup>, T. Grube<sup>a</sup>, B. Höhlein<sup>a</sup>, R. Peters<sup>a</sup>,  
A. Tschauder<sup>a</sup>

<sup>a</sup> Institute for Materials and Processes in Energy System (IWV 3), Forschungszentrum Jülich GmbH, D-52425 Jülich, Germany

<sup>b</sup> Haldor Topsøe A/S, Nymøllevej 55, DK-2800 Lyngby, Denmark

<sup>c</sup> Siemens AG, ZTEN1, D-91050 Erlangen, Germany

Accepted 24 November 1999

### Abstract

In the future, drive systems for vehicles with polymer electrolyte membrane fuel cells (PEMFC) may be the environmentally more acceptable alternative to conventional drives with internal combustion engines. The energy carrier may not be gasoline or diesel, as in combustion engines today, but methanol, which is converted on-board into a hydrogen-rich synthesis gas in a reforming reaction with water. After removal of carbon monoxide in a gas-cleaning step, the conditioned synthesis gas is converted into electricity in a fuel cell using air as the oxidant. The electric energy thus generated serves to supply a vehicle's electric drive system.

Based on the process design for a test drive system, a test facility was prepared and assembled at Forschungszentrum Jülich (FZJ). Final function tests with the PEMFC and the integrated compact methanol reformer (CMR) were carried out to determine the performance and the dynamic behaviour. With regard to the 50-kW(H<sub>2</sub>)-compact methanol reformer, a special design of catalytic burner was constructed. The burner units, with a total power output of 16 kW, were built and tested under different states of constant and alternating load. If selecting a specific catalyst loading of 40 g Pt/m<sup>2</sup>, the burner emissions are below the super ultra low emission vehicle (SULEV) standard. The stationary performance test of the CMR shows a specific hydrogen production of 6.7 m<sup>3</sup><sub>N</sub>/(kg<sub>cat</sub> h) for a methanol conversion rate of 95% at 280°C. Measurements of the transient behaviour of the CMR clearly show a response time of about 20 s, reaching 99% of the hydrogen flow demand due to the limited performance of the test facility control system. Simulations have been carried out in order to develop a control strategy for hydrogen production by the CMR during the New European Driving Cycle (NEDC). Based on the NEDC, an optimized energy management for the total drive system was evaluated and the characteristic data for different peak load storage systems are described. © 2000 Elsevier Science S.A. All rights reserved.

**Keywords:** Compact methanol reformer; Catalytic burner; Peak load energy storage; Fuel cell drive system; PEM fuel cell; Full fuel cycle

### 1. Introduction

On-board production of hydrogen from methanol, based on a steam reformer in conjunction with the use of low-temperature fuel cells, polymer electrolyte membrane fuel cells (PEMFC), is an attractive option as an energy conversion unit for light-duty vehicles. A steam reforming process at higher pressures, with an external burner, offers advantages in comparison to a steam reformer, with integrated partial oxidation, in terms of total efficiency for electricity production. The major aim of the Joule III project carried out by the Forschungszentrum Jülich (FZJ), Haldor Topsøe (HTAS), and Siemens AG is to design, to

construct, and to test a steam reformer reactor concept (HTAS), with external catalytic burner (FZJ) as heat source, as well as catalysts for heterogeneously catalyzed hydrogen production (HTAS), concepts for gas treatment (HTAS, FZJ), and a low-temperature fuel cell (Siemens). The subject of the following descriptions will be the test drive system, the experimental runs with the PEM fuel cell, the compact methanol reformer (CMR), and the choice of the peak load-energy storage.

### 2. Test drive system

The flowsheet worked out by FZJ, and shown in a simple version in Fig. 1, represents the basis for the

\* Corresponding author. Fax: +49-2461-61-6695.

E-mail address: b.emonts@fz-juelich.de (B. Emonts).

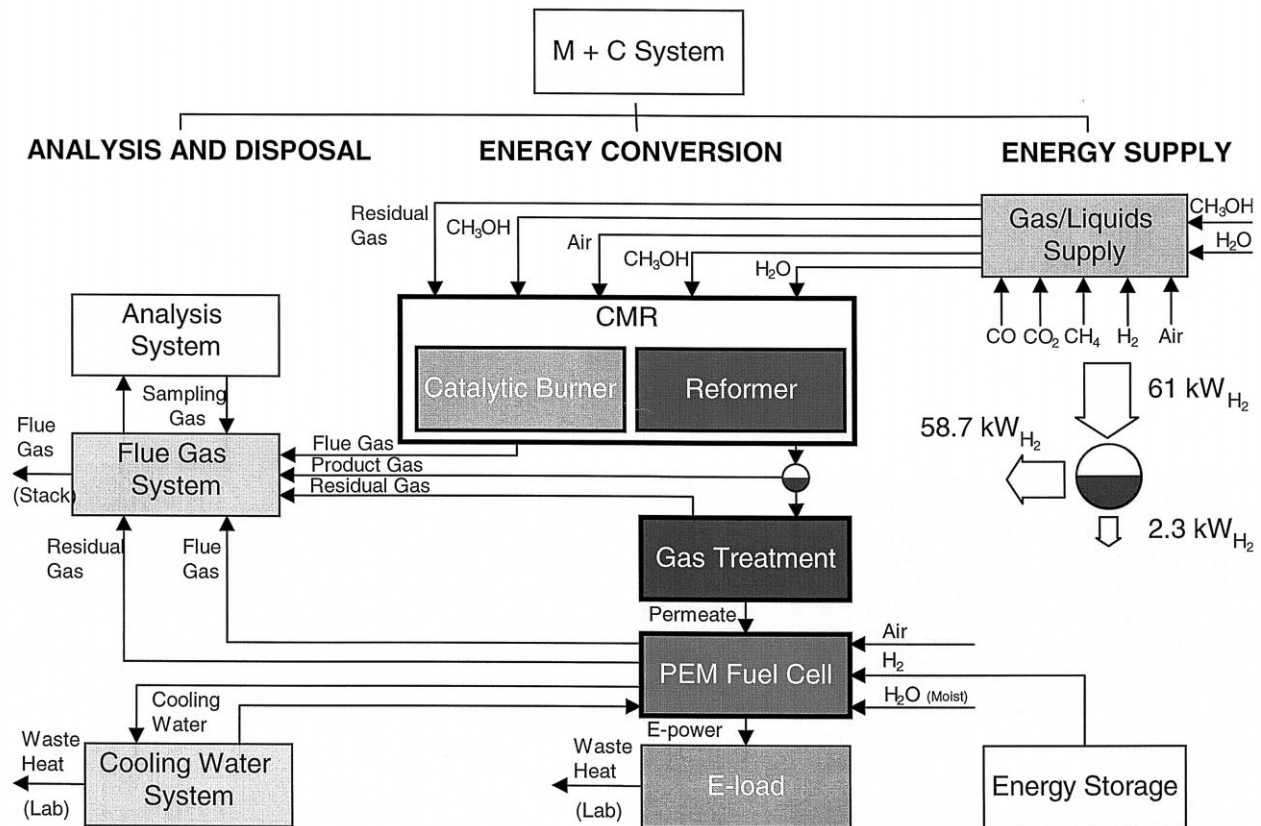


Fig. 1. Flowsheet of the test drive system.

process. Based on the specifications of HTAS and Siemens, and on the results of preliminary tests at FZJ, it takes account of all operating situations that can occur. For plant control, the process control system ‘Delta V’ from Fisher Rosemount was procured; this unit has more than 250 inputs and outputs and, moreover, ensures the integration of all devices. The entire data acquisition, process control, and process monitoring was carried out using this system.

An area of  $4.50 \times 3.60 \text{ m}^2$  was provided for the test facility in the small experimental hall of the FZJ/IWV-3. This area was also completely accessible from outside so that control elements could also be arranged at the edge of the area. The test facility occupied an area of  $2.00 \times 1.50 \text{ m}^2$ . The remaining area was needed for the control console, the switch cabinets, the analysis system, and the test gas supply. Fig. 2 shows a photograph of the complete test facility.

### 3. Experimental runs

#### 3.1. PEM fuel cell

The Siemens PEM fuel cell was investigated in a first set of experiments. The I/U characteristics were measured

for varying stack temperature ( $T$ ), hydrogen and air pressure ( $p_F$ ), nitrogen pressure ( $p(N_2)$ ), purge rate (PR), and air ratio ( $\lambda$ ), over the maximum range possible with the test stand. The I/U characteristics with the highest and lowest voltage for a given current are plotted in Fig. 3. The highest stack voltages were observed at a hydrogen and air pressure of 0.8 bar (g), a temperature of  $60^\circ\text{C}$ , an air ratio of 3.0, and a purge rate of 2.0. Current densities above  $120 \text{ mA/cm}^2$  could not be studied because the flow operation ranges of the flow controllers were chosen for a maximum power of 1 kW at an air ratio of 2.0 and a purge rate of 1.25. The lowest stack voltages were observed at a pressure of 0.49 bar (g), a temperature of  $35.1^\circ\text{C}$ , an air ratio of 2.0, and a purge rate of 1.5. The difference between both characteristics is lower at low power densities than at high current densities. The difference increases from 200 mV at  $8 \text{ mA/cm}^2$ , up to 350 mV at  $120 \text{ mA/cm}^2$ . It can be assumed that the influence of these parameters will increase further with increasing current density.

Further investigations describe the dynamic operation of the fuel cell. For this purpose, the performance characteristic of the New European Driving Cycle (NEDC) has been scaled by Grube [1] to the power range of the fuel cell used (see Fig. 4). For reasons of the controllability of the mass flow controller, however, a minimum power of 50 W

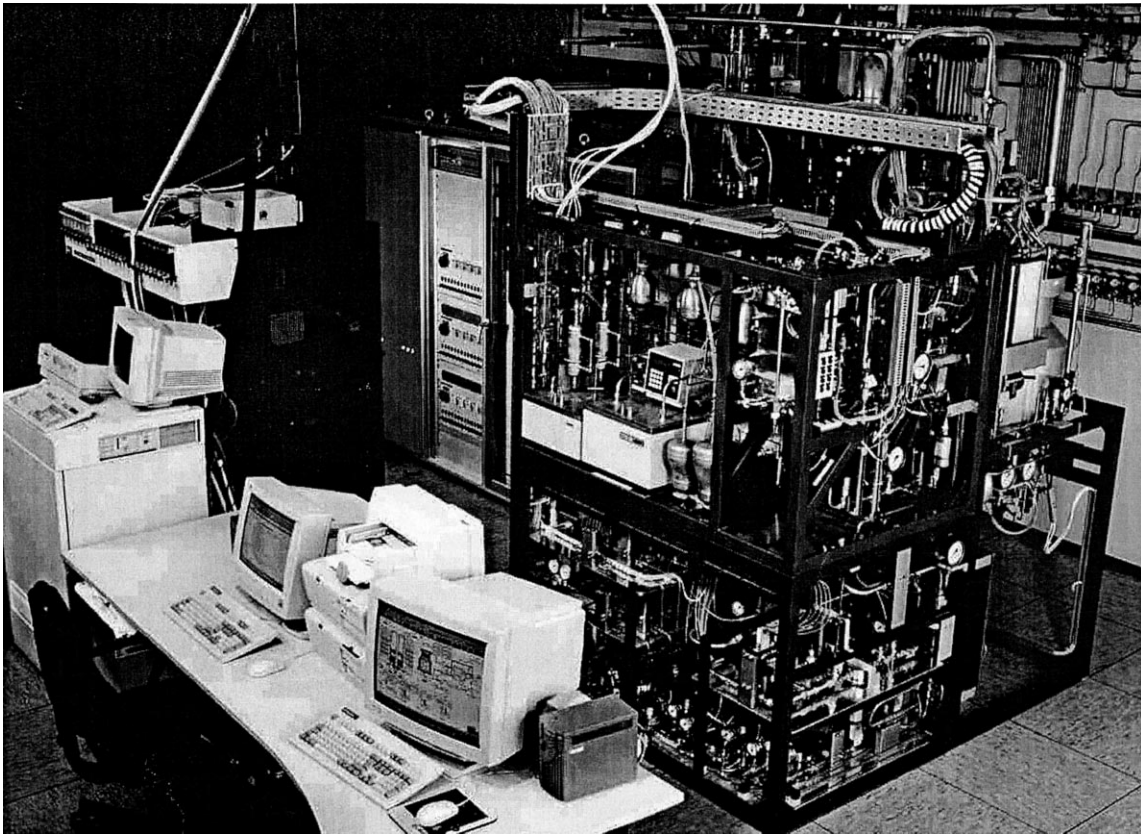


Fig. 2. Test facility.

was selected. This assumption is, moreover, in compliance with the electric power requirements of a real vehicle, since this permanently requires electrical energy for operating the ancillary components.

Essential parameters of the fuel cell, such as the hydrogen and air volume flow, current intensity, and overall voltage, were investigated. The mass flow controller thus supplies as much hydrogen to the fuel cell as is necessary.

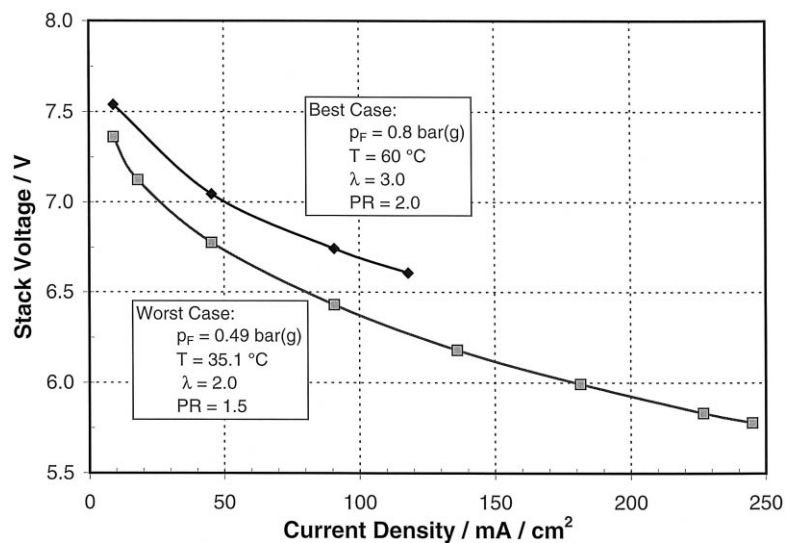


Fig. 3. Best and worst I/U characteristics.

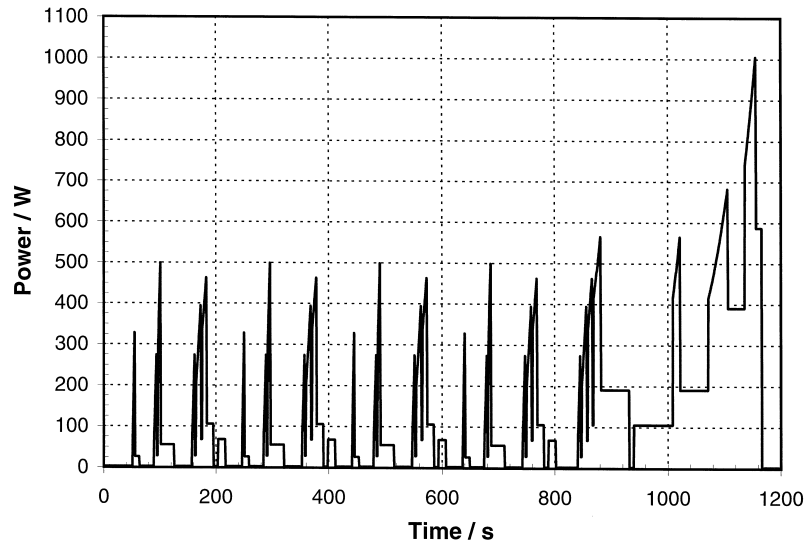


Fig. 4. Performance characteristic of the NEDC.

It can be shown, however, that the mass flow controller does not take up the new lower value sufficiently and rapidly. When plotting the hydrogen volume flow and the power over time, conformance is less pronounced. This is because the overall voltage drops with increasing current (see Fig. 5). In conclusion, it can be assumed that a load profile resembling a real traffic situation is feasible using the test rig.

### 3.2. Compact methanol reformer

The catalytic burner in the compact reformer has the function of providing the thermal energy required for the

reforming reaction, on the one hand, and of quantitatively converting all gases from the system, which still contains flammable fractions, into carbon dioxide and water on the other. The basic burner structure is a ceramic hollow cylinder to which fuel gas, premixed with air, is supplied internally. On the outer cylinder surface, a wire mesh, coated with noble metal is provided, on which the combustion reaction takes place catalytically. The burner structure has a density of  $311 \text{ kg/m}^3$  and the amount of catalyst on the wire mesh is  $40 \text{ g/m}^2$  for an active layer thickness of  $0.52 \text{ mm}$ .

On the basis of investigations of long-term stability, conversion of different fuels and flashback behaviour, a

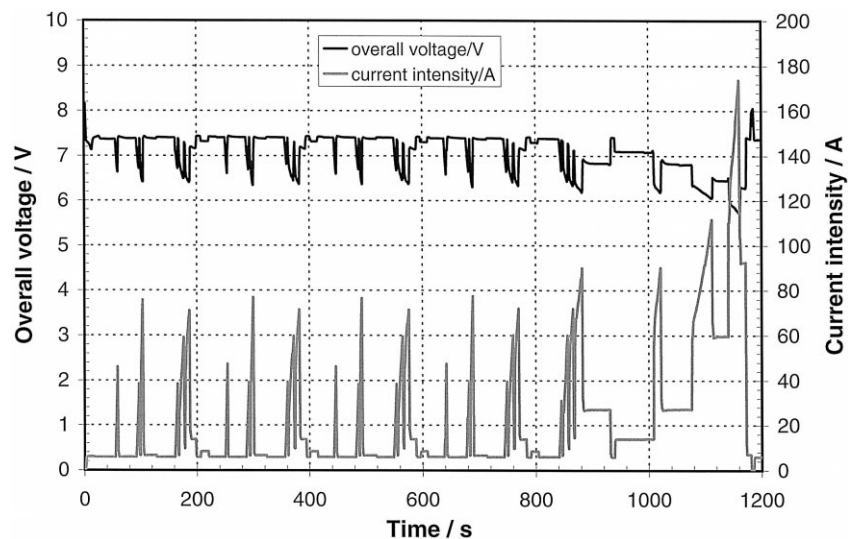


Fig. 5. Time characteristic of the overall voltage and current.

burner unit has been designed, constructed, and manufactured, for the compact reformer. The power density for the nominal load case was fixed at  $50 \text{ kW/m}^2$ . This value is a compromise. Higher power densities are favoured for the emission behaviour of the burner, since the temperature, and, thus, the conversion of the fuel gases, increases with rising power density. However, high power densities lead to a degeneration of the catalyst due to long-term factors indicated by high emission values. Lower power densities have a positive effect on flashback behaviour in addition to increasing long-term stability. In the case of a burner with a diameter of 80 mm, it is possible to accommodate six catalytic burners in an annular arrangement in the bottom section of the compact reformer. Since a total power output of 16 kW must be provided in the nominal load case, the height of the individual burners for optimum power density was determined as 212 mm.

Before the liquid methanol–water mixture can be fed into the reformer, the CMR has to be heated to its operating temperature, that is,  $260\text{--}280^\circ\text{C}$ , for the steam circuit and the reformer section. Therefore, methanol is fed into the catalytic burner to provide the heat demanded. For the catalyst, 3 kg of  $\text{Cu-Zn/Al}_2\text{O}_3$  have to be heated up from ambient temperature to  $260^\circ\text{C}$ . Assuming a heat capacity of  $0.8 \text{ kJ}/(\text{kg K})$ , it can be calculated that an energy difference of 564 kJ lead to a warm up time of about 47 s at a maximum thermal power of 12 kW from the catalytic burner. Unfortunately, mass of the steel casing with a heat capacity of  $0.477 \text{ kJ}/(\text{kg K})$ , also has to be heated up. For the worst case, 130 kg of the CMR must be heated to  $260^\circ\text{C}$ . These values lead to 16 MJ and a minimum warm up time of 22 min at a burner power of 12 kW.

Fig. 6 shows a realistic start-up of the CMR in the test-rig. The catalytic burner was fed with methanol for 3 min. Start-up takes 24 min for heating the steam circuit to

a temperature of  $300^\circ\text{C}$ , i.e., 27 min at the y-axis. While the steam circuit reaches its equilibrium value, the heat provided by the burner was reduced to 4 kW. The heating procedure cannot be accelerated due to the high temperature of  $571^\circ\text{C}$  at the catalytic burner. The upper limit is set to  $650^\circ\text{C}$  and must be matched by each of the six catalytic burners. The temperature shown in Fig. 6 is an average value of the six burners. Therefore, this temperature must be lower than the upper limit. After 27 min this temperature drops to  $350^\circ\text{C}$ . The temperature in the reformer increases much more slowly due to heat transfer from the steam circuit to the reformer tubes filled with catalyst. The liquid methanol flow controller can begin operation 36 min (39 min) after the catalytic burner at an inlet reformer temperature of  $250^\circ\text{C}$ . The temperature of the catalytic burners and the exhaust gases reach their equilibrium values of  $433^\circ\text{C}$  and  $183^\circ\text{C}$  respectively after 1 h. The heat provided by the burner amounts to about 6.5 kW. As can be seen, the initial assumptions about start-up are consistent with the experimental data. An improvement should be possible by reducing the thermal mass. The disadvantage of this steam circuit is a further retardation of 12 min.

Fig. 7 shows the start-up of the reformer. About 30 min after starting up the catalytic burner, the liquid flow controllers were activated to deliver methanol and water into the reformer; the reformer inlet temperature was  $225^\circ\text{C}$ . A further 4 min was necessary to obtain product flow at the reformer exit. This period was needed to fill a buffer vessel with the liquid feed mixture. This buffer was installed to protect the flow controllers against pressure fluctuations arising from the evaporator. This additional vessel will need to be optimised in future.

The compact methanol reformer has been operated in a test mode at  $260^\circ\text{C}$  and  $280^\circ\text{C}$  up to theoretical hydrogen production rates of  $5 \text{ m}^3_{\text{N}}/(\text{kg}_{\text{cat}} \text{ h})$  and  $7 \text{ m}^3_{\text{N}}/(\text{kg}_{\text{cat}} \text{ h})$ ,

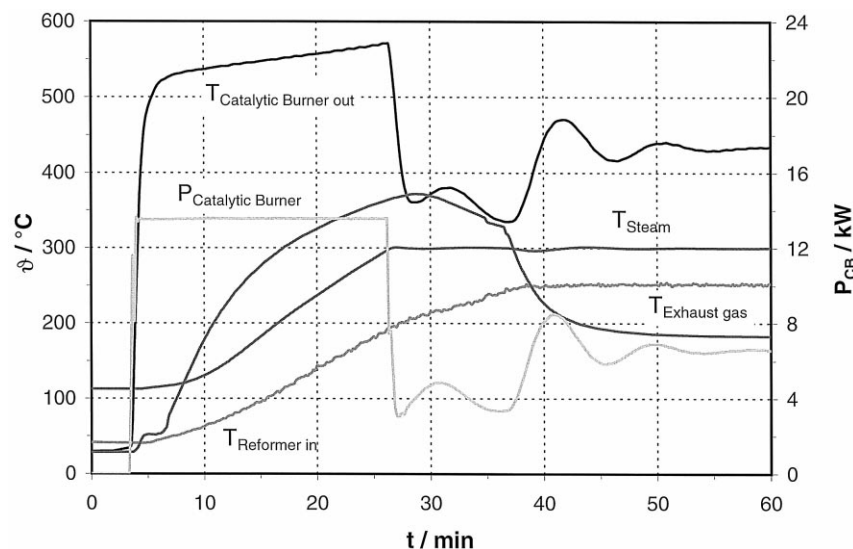


Fig. 6. Starting up the catalytic burner and the steam circuit.

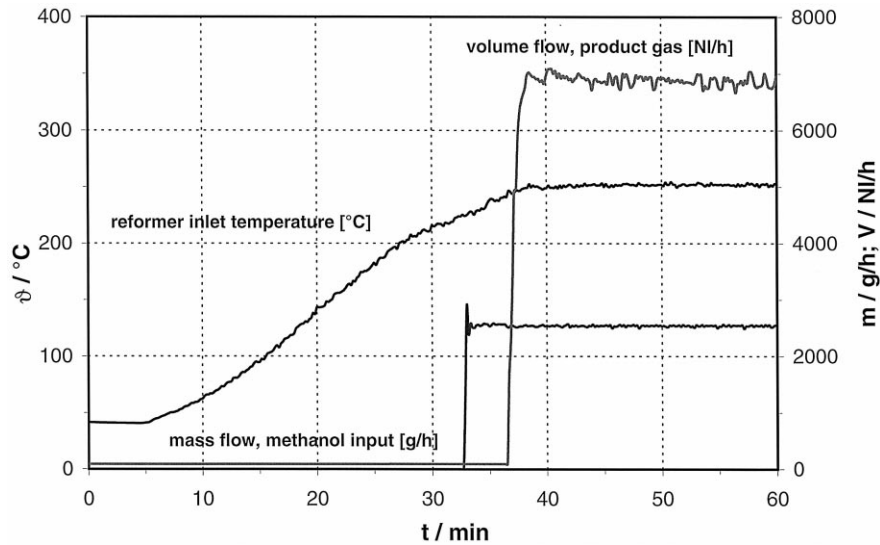


Fig. 7. Starting up the reformer.

respectively. In order to connect the Pd-membrane, the system pressure was chosen as 21 bar. The compact methanol reformer performance was compared, in terms of methanol conversion, and dry CO concentration, with experiments for a single tube filled with a catalyst loading of 25%, that is, a catalyst mass of 35.5 g in a tube 25 cm in length and a diameter of 12.2 mm. These dimensions correspond to those of the CMR.

In Fig. 8, the methanol conversion rate is plotted as a function of the theoretical specific hydrogen for the CMR, and for a single reactor tube at two temperatures, i.e., 260°C and 280°C. The methanol conversion rates of the

CMR are somewhat lower than those for the single tube under a comparable load, that is, an equal theoretical specific hydrogen production. At 280°C, a methanol conversion of 95% is achieved at a theoretical production rate of  $6.7 \text{ m}_N^3/(\text{kg}_{\text{cat}} \text{ h})$  for the CMR and  $7.87 \text{ m}_N^3/(\text{kg}_{\text{cat}} \text{ h})$  for the single tube. The high pressure of 21 bar for the CMR experiments leads to a lower equilibrium conversion. The equilibrium methanol conversion can be determined as 99.2% at 280°C and 98.1% at 260°C. The experiments clearly show a limitation in the methanol conversion at low loads and higher pressures. The methanol conversion rate for the CMR provides 86% of the design value

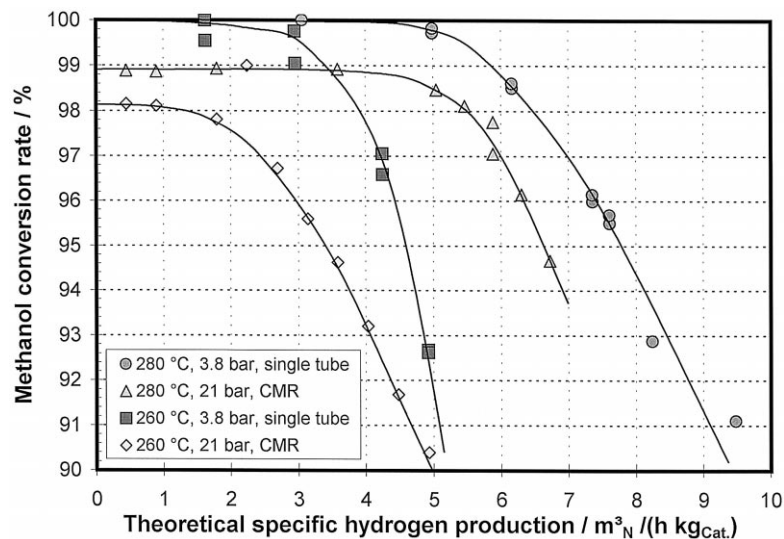


Fig. 8. Methanol conversion as a function of specific hydrogen production for the CMR and a single reactor tube; molar water/methanol ratio ( $M$ ) 1.5; mixture density ( $\rho$ ) 0.905 kg/l (25°C).

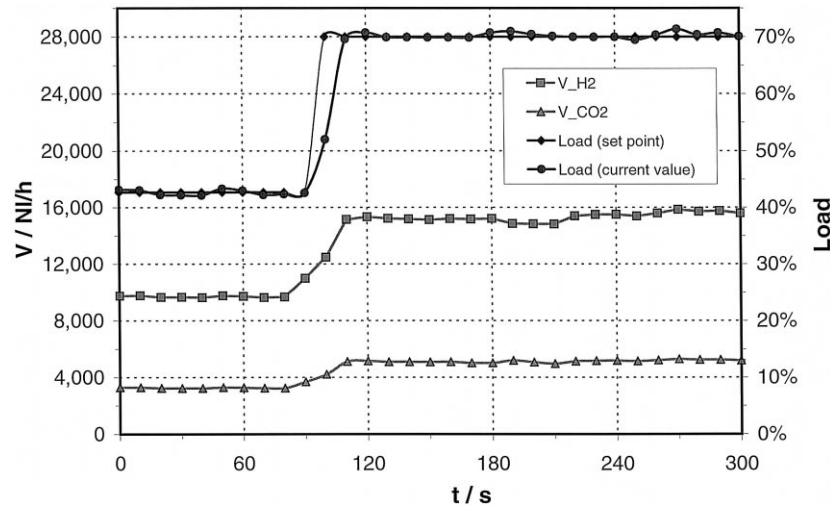


Fig. 9. Transient behaviour of the CMR for product flow; load change from 40% to 70% at 280°C;  $M = 1.5$ ;  $\rho = 0.905 \text{ kg/l}$  (25°C).

derived from experiments with single tubes. Taken into account that the CMR consists of a bundle of tubes, the efficiency of such a scale-up is very satisfactory.

In the following section, the CMR performance with respect to transients is discussed. The experiments were performed by load changes, for example, from 5% up to 10%, from 10% up to 20%, from 20% up to 40%, and from 40% up to 70%. These partial loads are related to the maximum flow of the methanol liquid flow controller. The partial loads, related to the design value of the CMR, are higher by a factor of 1.15; for example, the load change of the liquid flow controller from 40% up to 70% gives rise to a load change of the CMR from 46.1% up to 80.7%. Fig. 9 shows the signal of the control system for the methanol liquid flow controller, the resulting methanol

flow passing into the reformer and the response functions for the hydrogen and the carbon dioxide outflow of the CMR. The signal to the liquid flow controller for methanol changes over a time interval of 10 s. The change in the input flow of methanol is stabilized after a period of 20 s. The hydrogen and the carbon dioxide flow at the reformer exit follow the input flow of methanol spontaneously, without any delay. As in the case for the transient experiments reported by Dusterwald [2], the hydrogen flow is determined by the transients in the delivery system for the inlets.

In the next section, the energy balance of the CMR is discussed. Fig. 10 shows the efficiency of the CMR as a function of the partial load of the CMR for the liquid methanol flow into the reformer at 260°C and 280°C. This

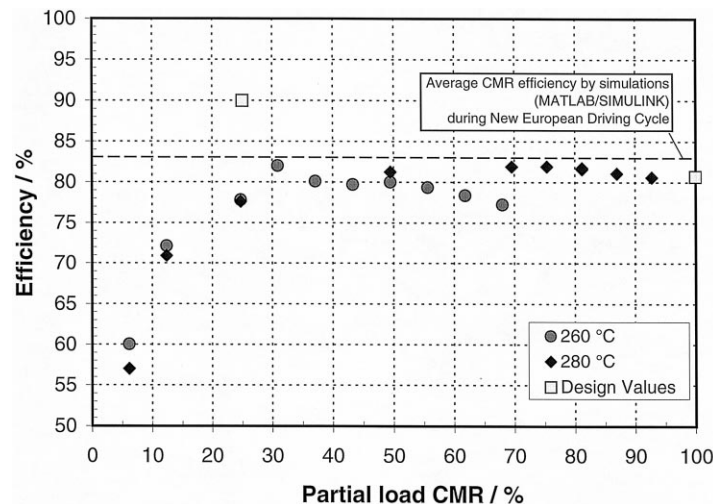


Fig. 10. Efficiency of the CMR during stationary operation.

efficiency is defined as the ratio of the enthalpy flow (lower heating value, LHV) of hydrogen exiting the reformer to the input enthalpy flow (LHV) of methanol and the heating values of the burner fuel. During the first tests of the CMR, the catalytic burner is fed with methanol and partly with hydrogen; for the balance of plant calculations performed by HTAS, it is assumed that the catalytic burner will be fed with hydrogen, methanol, methane, and carbon monoxide, coming from the gas clean-up system and the fuel cell. The efficiencies from these BoP calculations amount to 80.7% at full load and 90% at 25% partial load. Additional calculations with a dynamic simulation tool for the fuel processing system in the NEDC result in an average efficiency of 87%. In Fig. 10, the efficiency calculated from the measured flows from the test facility clearly shows a dependence on load. Starting at a low partial load of 6%, the efficiency of the CMR is 60%. At 25% load, the efficiency increases up to 78%, which is near the value of 80% for partial loads between 50% and full load. At a temperature of 260°C, the efficiency slightly decreases with increasing load due to a decreasing methanol conversion rate. The efficiency of the CMR is at a maximum of 82% at 280°C for a load between 70–80%, somewhat higher than the design value. The lower efficiency at lower loads would be circumvented by a step-wise fuel inlet control of more than two reformer units, as indicated in the simulation calculations by Dusterwald [2] and Peters et al. [3].

#### 4. Peak load energy storage

Compressed gas storage systems, batteries, supercapacitors, and flywheels, are possible for peak load storage. They differ considerably in terms of energy density (W h/kg, W h/l), power density (W/kg, W/l), charge and discharge (cycles, time, energy demand), availability, and costs. Only batteries, flywheels, and supercapacitors, can be used for regenerative braking. It is apparent that the state-of-the-art, with regard to flywheels, is presently insufficient; supercapacitors can provide high power for a short time and batteries provide more energy, if compared with storage systems of the same weight. To provide a power train in a dynamic operating cycle with an additional 1 kW h, a battery would weigh 20 kg, on average, at a best-case power level of 6 kW, which would not be sufficient for the peak load of a passenger car. On the other hand, a supercapacitor for 30 kW peak power would weigh 20 kg in the best case, with an energy supply up to 100 W h, which, in turn, is not sufficient for the peak load of the power train. Additional weight for the power train in the form of storage systems costs additional specific energy; 100 kg more power train weight will cost an additional 5–10 MJ/100 km or up to 0.3 l of gasoline-equiv-

alent. Within the framework of this project, it was decided to integrate a gas storage system. With this system, regenerative braking is not possible, but the clean hydrogen production in fuel processing allows this hydrogen to be stored in an efficient way using it for peak loads as well as for start-up procedures of the total power train.

The power train simulation, shows that, at the end of the driving cycle, the filling level is lower than the nominal filling level. The storage system must be replenished during a coasting period. This means that the fuel cell system is in operation but does not provide any drive power. This can significantly influence the energy balance of the vehicle, depending on the storage strategy and system management.

#### 5. Conclusions

Based on the specifications of the partners, on the process design and on the results of preliminary tests at FZJ, a test drive system was prepared and assembled. To investigate the behaviour of the units delivered by the partners, final function tests were carried out. Thus, the influence of different parameters on the PEM fuel cell performance and dynamic operating behaviour were studied. Such load profile that could arise in a real traffic situation is feasible at the test site. Based on preliminary studies and experiments, a catalytic burner unit was designed, constructed and manufactured for the CMR. In the case of a burner diameter of 80 mm, it is possible to accommodate six catalytic burners with a total power output of 16 kW in an annular arrangement in the bottom section of the CMR. A pre-screening carried out by Schneider [4] of the performance shows that the burners fulfil the super ultra low emission vehicle standard (SULEV) if the specific amount of catalyst totals 40 g Pt/m<sup>2</sup>.

For the CMR, experiments in single reaction tubes were undertaken to obtain better data for the reformer design and to study different operating modes. Afterwards, a CMR test was carried out to determine the reformer performance and the dynamic behaviour. The stationary performance test of the CMR showed a specific hydrogen production of 6.7 m<sup>3</sup><sub>N</sub>/(kg<sub>cat</sub> h) for a methanol conversion rate of 95% at 280°C. Measurements of the transient behaviour of the CMR clearly show a response time of

Table 1  
Comparison of measurement results and SULEV standard

Emissions	Pre-experimental results (mg/km)	SULEV standard (mg/km)
CO	0.3	625
NO <sub>x</sub>	< 0.01	12
VHC	0.9	6



about 20 s for 99% hydrogen flow demand due to the limited performance of the test facility control system.

The basis for a comparison of different power trains is the NEDC (see Table 1). Since different units of the power train differ in dynamic behaviour, a short-term storage system for peak load storage will be necessary. Therefore, the characteristic data for compressed gas storage systems, batteries, supercapacitors, and flywheels, will need to be examined. Within the framework of this project, it was decided to integrate a gas storage system.

## References

- [1] T. Grube, Diploma work, FH Aachen, Germany, 1998.
- [2] H.G. Düsterwald, PhD thesis, RWTH Aachen, Germany, 1997.
- [3] R. Peters, H.G. Düsterwald, B. Höhle, Proc. 31st ISATA, Düsseldorf, Germany, 2–5 June 1998.
- [4] P. Schneider, Diploma work, FH Aachen, Germany, 1999.